Relationship between Aircraft Design and Flight-Measured Loads

W. T. WITTEL* AND T. E. DISNEY†
Lockheed-Georgia Company, Marietta, Ga.

A critical review of current structural design criteria, analysis methods, and data handling techniques is presented, summarizing practices that are known to result in large discrepancies between design loadings and those that actually occur in flight. Alternate criteria, methods, or research programs are suggested which would serve to eliminate or reduce these discrepancies. Particular emphasis is placed on contemporary methods of providing structural integrity for flight in the stall buffet regime, and a rational method is derived for predicting empennage loads at stall. The method involves the superposition of quasi-static airloads at the stall with incremental dynamic inertia loadings derived from wind-tunnel data. Design loadings resulting from application of the method are compared with loads measured during flight tests of a large, swept-wing, high subsonic transport. The results indicate that empennage buffet loads can be satisfactorily predicted when suitable wind-tunnel data are available, and that the use of the arbitrary factors required by the current military design criteria results in loadings that are too high in the root regions and too low in the tip regions of the empennage.

Nomenclature

L_{net}	= net load
$(L/nW)_q$	= additional load at a given q
nW	= load factor times weight, lb
$(L @ n_z = 0.0)_q$	= basic load at a given q
V_q	= voltage readouts at a given q for $n_z = 0.0$
$(V @ q = 0.0)$	= strain gage zero voltage
L/V	= strain gage sensitivity in load/v, determined by ground calibration
$L_{1.0g}$	= net load on the ground, i.e., 1.0-g inertia load
ΔV	= incremental voltage change
q_t	= dynamic pressure at the trim point, psf
C_{L_t}	= horizontal tail lift coefficient
α_{FRL}	= fuselage angle of attack, deg
ϵ	= downwash angle, deg
i_t	= stabilizer incidence angle, deg
δ_e	= elevator deflection, deg
$C_{L\delta_e}$	= lift coefficient/deg elevator
$C_{L\alpha_t}$	= horizontal tail lift curve slope/deg
q	= dynamic pressure, psf
S	= horizontal tail area, ft^2
$(cc_{1b}/c_{av})_\eta$	= spanwise basic loading-airload distribution when the total horizontal tail airload is zero
$(cc_l/C_{L_t}c_{av})_\eta$	= spanwise additional loading, normalized to unit lift coefficient
$S_{Z\eta}$	= airload shear, lb
$M_{X\eta}$	= airload bending moment, in.-lb
$M_{Y\eta}$	= airload torsion moment, in.-lb
b	= horizontal tail span, in.
ΔX	= distance from local aerodynamic center to load reference axis, in.
$\bar{C}$	= horizontal tail mean aerodynamic chord, in.
η	= nondimensional spanwise ordinate $2Y/b$
Y	= spanwise station, in.
$(S_Z/\Delta n_{z\text{tip}})_\eta$	= unit shear loading, lb/g
$(M_X/\Delta n_{z\text{tip}})_\eta$	= unit bending moment loadings, in.-lb/g
$(M_Y/\Delta n_{z\text{tip}})_\eta$	= unit torsion loading, in.-lb/g
$(W)_\eta$	= local panel weight, lb
$(n_z)_\eta$	= local load factor derived from normalized 7.0 cps symmetrical bending mode shape (see Fig. 9)
$(\Delta X)\eta$	= distance from panel c.g. to reference axis, in.

Presented as Paper 66-881 at the AIAA Third Annual Meeting, Boston, Mass., November 29–December 2, 1966; submitted November 7, 1967; revision received May 29, 1967. [6.01]

* Aircraft Structures Engineer, Senior.
† Loads Group Engineer.

Introduction

THIS paper discusses several of the more important areas where criteria, analysis methods, or data reduction techniques are known to have resulted in significant differences between predicted and flight-measured loads on the C-141 airplane. With one exception, all of the areas are discussed in terms of the effect on empennage loads, since the effects on other components are secondary in nature. The one exception involves the wind-tunnel testing techniques which primarily affect the wing loadings, although the secondary effect on the empennage due to the change in airplane balance is quite significant.

The discussions that follow are broken down into the broad areas of "Criteria" and "Analysis Methods." All of the criteria items are interrelated in terms of the effects on empennage loads; this is especially true where the criteria for abrupt checked pitch maneuvers, and unsymmetrical horizontal tail loads in the aerodynamic stall regime are concerned. Alternate criteria for abrupt checked pitch maneuvers are suggested, and a rational method of predicting horizontal tail loads in the stall regime is developed.

Two analysis methods are discussed: the method of establishing flight test zeros resulted in significant errors in the flight-measured horizontal tail loads, but did not noticeably affect the wing loads; hence, the discussion is centered around the horizontal tail effects although the proposed alternate method of handling the data is equally adaptable to wing loads. The wind-tunnel testing techniques are discussed in terms of the effects on the wing, although, as previously mentioned, large discrepancies in the balancing horizontal tail load are caused by the errors introduced into the wing load by the present techniques. Intuitively, if the wind-tunnel testing techniques are modified so that correct results are obtained for the wing, the horizontal tail load discrepancies will disappear.

Criteria

The following discussion of structural design criteria involves only those items that are known to have caused significant discrepancies between design loads and flight-measured loads on the C-141 airplane, and is in no way intended to be a critical review of all structural design criteria.

Abrupt Checked Pitch Maneuvers

The military structural design criteria require that the final elevator deflection reached in the check phase of the abrupt symmetrical pitch maneuver occur simultaneously with the attainment of peak load factor. A literal application of this requirement may result in design horizontal tail loads which greatly exceed those actually occurring in flight for two reasons. First, the requirement may be inconsistent with the response characteristics of large airplanes with fully powered control systems in that it may be physically impossible to obtain the required relationship without pitching the airplane to extreme attitudes well beyond the range normally considered for limit design load conditions. Second, flight test demonstration requirements do not specify coincidence of peak load factor and elevator return; consequently, the maneuver is performed using the minimum elevator deflection that will yield the required load factor by the specified deflection time history, regardless of the time-phase relationship of elevator position and peak load factor.

The C-141 is a good example of an airplane for which the present criteria resulted in design load levels that grossly exceeded the maximum flight-measured loads. Part of the excessive design load resulted from the use of arbitrary unsymmetrical horizontal tail load requirements, which will be discussed in detail elsewhere. The remainder of the excessive load, however, is directly attributable to the wording of the abrupt checked pitch maneuver requirement.

In order to obtain coincidence of elevator return and peak load factor during the analytical design load analysis it was necessary to pitch the C-141 airplane to an angle of attack well beyond that for the maximum wing lift. This could be done without exceeding the 2.5-g design maneuver load factor at speeds up to, and including, the 2.5-g stall speed since the load factor ceased to increase with angle of attack after the maximum lift coefficient was reached. The horizontal tail load, on the other hand, continued to increase, since the horizontal tail stalls at a much higher airplane angle of attack than the wing, because of the effects of downwash and horizontal stabilizer incidence. Figure 1 illustrates a typical series of analytical time histories for an abrupt pitch maneuver with the elevator checked to a position equal to one-half the input deflection and opposite in sign. The (a) curves represent a minimum response type of elevator input where the initial elevator deflection is equal to that required for a balanced maneuver at the required load factor. The (b) curves represent an intermediate elevator deflection, and the (c) curves represent an extremely violent maneuver which will pitch the airplane to an angle of attack several degrees higher than that required for maximum lift. The fully powered control system of the C-141 was rate limited by the power output of the actuators and could not produce sufficient elevator deflection rates to obtain coincidence of elevator return and peak load factor for the maneuvers indicated by the (a) and (b) curves. It was necessary, therefore, to go to the (c)-type input in order to pitch the airplane into the deep stall regime where the delay in load factor decay would allow sufficient time for elevator return to be accomplished. The resulting horizontal tail loads were approximately twice the magnitude of the largest flight-measured loads. The design horizontal tail loads showed an even greater discrepancy because of the requirement for applying the arbitrary 1.50 factor, which is discussed in the following section. The net result was a design load level, which was approximately three times the magnitude of the highest measured load.

From the foregoing discussion it is obvious that the military requirement for coincidence of elevator return and peak load factor can result in severe weight penalties to the airframe. It appears that the way in which this problem can be overcome is to eliminate the requirement for coincidence. With this in mind, it is suggested that the most realistic criteria would consist of designing the structure to accommodate loadings compatible with the manner in which the airplane will be flown. That is to say, the specification should only state the manner in which the elevator control, at the flight station, is to be displaced, and the final load factor that must be reached. The time-phase relationship of peak load factor to final elevator deflection should not be a consideration.

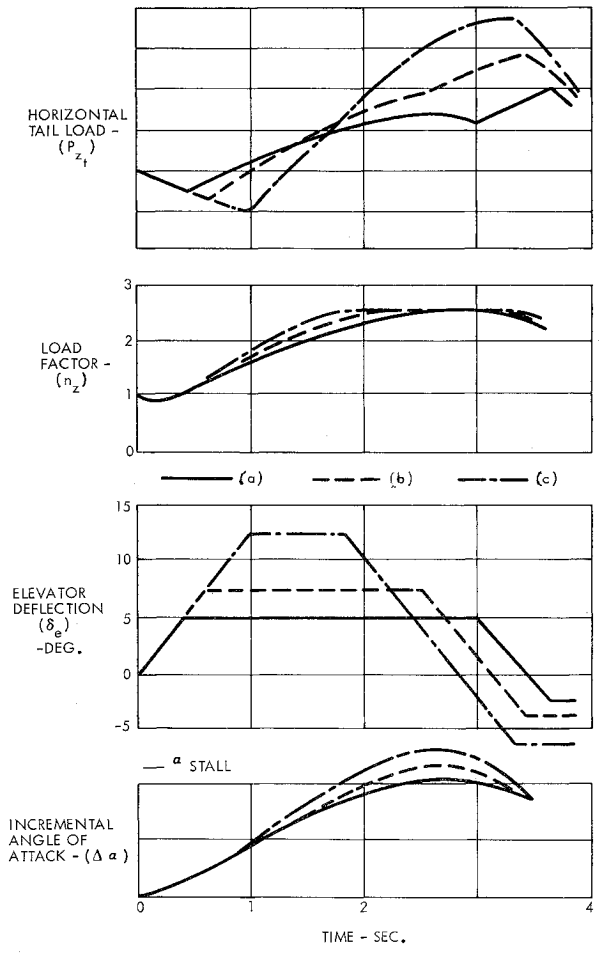

Fig. 1 Analytical time histories of abrupt checked pitch maneuvers.

Unsymmetrical Horizontal Tail Loads

Current structural design criteria require the application of arbitrary distribution factors to the horizontal tail loads resulting from symmetrical flight conditions. There is a tremendous disparity between the civil and military requirements in this respect. The civil criteria require a 10% asymmetry, obtained by multiplying the net load on one side of the horizontal tail by 1.0 and that on the other side by 0.80, throughout the flight regime. The military criteria require a 100% asymmetry, obtained by multiplying the airload on one side of the horizontal tail by 1.50 and that on the other side by 0.50, at all points in the flight regime representing aerodynamic stall, along with a 30% asymmetry, obtained by factors of 1.15 and 0.85, at all other points in the flight regime. The disparity is readily apparent since the military criteria result in a 50% increase in the design load level on one side of the horizontal tail in the stall regime, and a 15% increase at all other points in the flight regime. The civil criteria, on the other hand, do not cause any increase in the design horizontal tail loads.

The relative merits of the two sets of criteria are not in contention here. In fact, it can be shown that neither set of criteria is adequate in the stall regime. The use of the 1.0–0.8 factors required by the civil criteria may result in

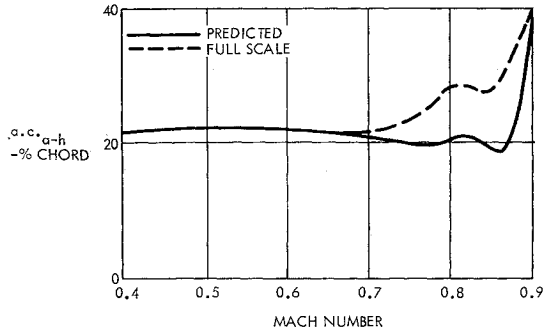

Fig. 2 Comparisons of predicted and full-scale aerodynamic center locations.

structure which is greatly understrength, whereas the use of the 1.50–0.50 factors required by the military criteria results in loads that are too high in the root region and too low in the tip region of the horizontal tail. A rational method of predicting empennage loads in the stall regime is presented in the section on empennage loads due to stall buffet, which is recommended as a substitute for the subject arbitrary factors.

As far as the factors that are applied at speeds in excess of stall are concerned, it appears that additional research is needed. A wealth of experimental data is readily available in the form of airloads surveys on the many Air Force airplanes which have been flight tested, and it requires only the expenditure of sufficient time and effort in studying these data to arrive at a realistic asymmetry factor.

Center of Gravity Position for Structural Design

Military structural design criteria require an arbitrary center of gravity tolerance band of 1.5% of the mean aerodynamic chord, or 15% of the distance between the actual most-aft and actual most-forward centers of gravity, whichever is the greater. Application of this requirement results in design loads that exceed those actually occurring in flight. Since excessive design loads intuitively mean excessive weight and increased cost, this requirement should be carefully weighed in order to evaluate its necessity.

Apparently the arbitrary center of gravity tolerance was originally intended primarily for fighters and other types of airplanes with small design center of gravity ranges. In any case, it has very little application to large transport aircraft which have a good measure of center of gravity control available in the form of cargo.

For the design of transport category aircraft it is suggested that the arbitrary center of gravity tolerance be eliminated and replaced by rational considerations of longitudinal center of gravity movement, resulting from fuel redistribution due to airplane attitude.

Analysis Methods

Establishing Flight Test Zeros

During the C-141 flight test program, horizontal tail loads were measured in two ways; by integrating measured pressure data, and by direct strain gage readouts. The integration of the measured pressure data closely agreed with predicted loads at low Mach numbers, whereas the strain gage data indicated loads which were significantly higher than predicted. This apparent discrepancy was traced directly to the method used in establishing strain gage zeros.

Strain gage zeros have traditionally been established by flying a series of zero-g maneuvers at several airspeeds and a constant Mach number, plotting the strain gauge voltage readouts as a function of dynamic pressure, and extrapolating the results to zero airspeed. Intuitively, the net load is zero when both the load factor and airspeed are zero; consequently, any strain gage voltage reading which exists for the specified condition represents an anamoly, which is commonly designated as the "strain gage zero."

The strain gage zero is used in the reduction of net loads as follows:

$$L_{\text{net}} = (LnW)_q(nW) + (L@n_z = 0.0)_q \quad (1)$$

$$(L@n_z = 0.0) = [V_q - (V@q = 0.0)]L/V \quad (2)$$

An alternate method of establishing net load magnitudes from measured strain gage voltages consists of using the instrumented flight test airplane as its own calibration device. To accomplish this end, strain gage voltages are read while the airplane is resting on the ground, immediately followed by flying to a preselected low-speed, low-altitude trim point, and reading the incremental change in strain gage voltage. The actual load magnitude can then be calculated for the preselected trim point very accurately since the only factors to be considered are the known values of the 1.0-g load on the ground and the strain gage calibration in terms of load per volt as follows:

$$L_{\text{net}} = L_{1.0g} + L/V(\Delta V) \quad (3)$$

Once the load level at the preselected trim point is established by the method indicated by Eq. (3), the strain gage zero value can be removed from Eq. (2) by equating (3) and (1) at the q corresponding to the preselected trim point as follows:

$$(L/nW)_{q1}(nW) + (L@n_z = 0)_{q1} = L_{1.0g} + L/V(\Delta V) \quad (4)$$

The use of Eq. (4) allows the basic load level to be established at the q corresponding to the preselected trim point and hence the strain gage zero value can be eliminated from consideration.

Reaching the preselected trim point as quickly as possible cannot be overemphasized, since doing so minimizes the errors introduced by the effects of temperature on the structure, and hence the strain gage output. Once the load level at the low speed trim point has been definitely established for each flight, it can be used as a base point for all other measurements.

Wind-Tunnel Testing Techniques

The current methods employed in wind-tunnel testing and data analysis appear to be inadequate for determining accurate aerodynamic data for structural design of high subsonic speed transport-type aircraft. This conclusion is based on differences between full-scale C-141A flight test derived data and wind-tunnel derived aerodynamic data. These discrepancies in aerodynamic data occur in the high subsonic speed range and have been traced to an unsuspected effect of Reynolds number on the shock boundary-layer interaction. The full-scale shock locations in the mid span region of the C-141A wing are from 10 to 15% farther aft than those predicted from wind-tunnel test results. This difference in shock location results in significant errors in local aero-

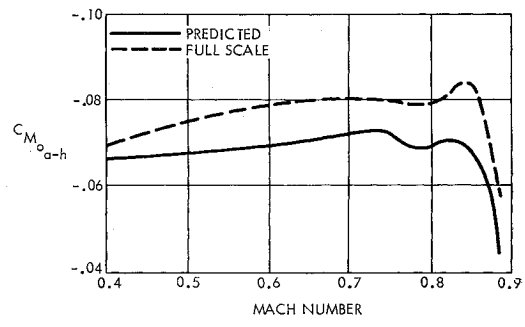

Fig. 3 Comparison of predicted and full-scale $C_{M_{0_{a.h}}}$ values.

dynamic center locations, zero-lift pitching moments, and spanwise lift distributions. A comparison of full-scale and wind-tunnel derived tail-off aerodynamic center and the zero-lift pitching moment coefficient is shown in Figs. 2 and 3.

It is obvious that some means must be available in a wind-tunnel test program to obtain the form of shock boundary-layer interaction that will occur on the airplane in order to obtain model force data consistent with known full-scale turbulent boundary-layer conditions. It has become standard practice to artificially trip the boundary layer on the model in order to accomplish this objective.

Early in the C-141 development program, Lockheed conducted wind-tunnel studies of the effects of "fixing" transition and found significant changes in model lift, pitching moment, and drag coefficients. Consultations with various authorities confirmed that the "fixed" transition results would more nearly define the full-scale forces. Extensive wind-tunnel studies were conducted in various transonic tunnels to determine the effects of Reynolds number on aerodynamic data obtained from both fixed and "free" transition testing. Figure 4 illustrates typical results obtained from these tests on tail-off zero-lift pitching moment at a Mach number of 0.825. The tendency of fixed and free transition data to converge with increasing Reynolds number indicated that, if tests were conducted at sufficiently high Reynolds numbers, it would be unnecessary to fix transition in order to approximate full-scale effects. Since the majority of C-141 wind-tunnel tests were, of necessity, conducted at low Reynolds number, the fixed transition testing technique was used. A comparison of model and full-scale shock locations on the C-141A wing is shown in Fig. 5.

The two data sources show good agreement at the wing root and tip where flow is predominately three dimensional. The large discrepancies occur in the region where the flow is most nearly two dimensional. Extensive analyses of fixed and free transition model pressure data over a range of Reynolds numbers of 1.5 to 5 $\times$ 10^6 indicate that the root and tip shock location is relatively independent of the condition of the boundary layer, whereas the midspan locations show a forward shift of shock position with fixed transition. It therefore appears that a significant scale effect exists where the model boundary layer is laminar or has been modified by fixing transition, which may introduce additional scale effects. Lockheed is currently investigating this problem in collaboration with NASA Ames, Langley, and several United Kingdom organizations.

Empennage Loads Due to Stall Buffet

Background

During the flight test stall demonstrations of the C-141 airplane, high loads were measured on the outer span of the horizontal tail when angles of attack exceeding that for maximum wing lift were reached. In some cases the load magnitudes exceeded the design limit strength by a considerable

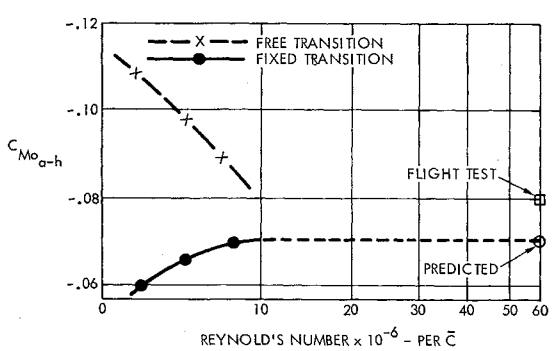

Fig. 4 Effect of Reynolds number on $C_{M_{0_{a-h}}}$ at Mach 0.825.

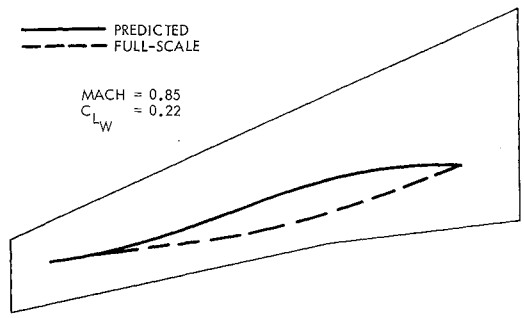

Fig. 5 Comparison of predicted and full-scale shock locations.

margin. Figure 6 shows a comparison of the maximum measured horizontal tail bending moment. The comparison clearly shows a major difference between the measured load distribution and the predicted distribution, which was derived from the application of the traditional multiplying factors to the quasi-static airload.

Examination of flight test measured horizontal tail load and tip load factor data showed that the excitation of the horizontal tail was strongly influenced by airplane configuration. In the clean configuration the horizontal tail responded in a 7.0-cps symmetric bending mode; whereas, when the flaps were down, a 4.0-cps antisymmetric mode was excited. In either case, the magnitude of the excitation was found to be primarily a function of airplane angle of attack, airspeed, and altitude. As airplane angle of attack was increased in an approach to stall, the horizontal tail began to buffet at approximately 11.0°. The buffet increased in severity until approximately 20.0° was reached. At angles of attack in excess of 20.0° the buffet magnitude decreased. This trend is easily explained by the location of the C-141 horizontal tail relative to the wing. The T-tail configuration places the horizontal tail in relatively clean flow until the airplane is pitched up to an angle where the horizontal tail begins to enter the wing wake. The downwash from the wing keeps the major portion of the wake below the horizontal tail until wing stall occurs. When the wing stalls, the sudden decrease in downwash, coupled with the fact that the angle between the C-141 wing and horizontal tail is approximately equal to the stall angle of attack, places the tail directly in the turbulent wake of the wing. It follows that the degree of turbulence in the wing wake also increases sharply when stall occurs. As the airplane continues to pitch up to angles of attack in excess of 20.0°, the horizontal tail begins to move below the wing wake and consequently the degree of buffet decreases. Figure 7 helps to illustrate this relationship.

Flight test measured loads data showed that the largest horizontal tail loads occurred in the clean configuration.

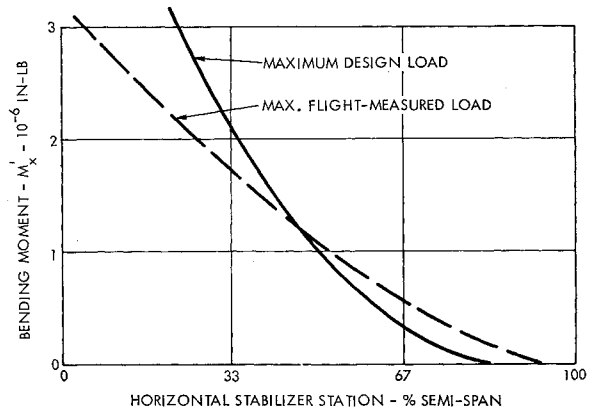

Fig. 6 Comparison of maximum predicted and flight-measured horizontal tail load.

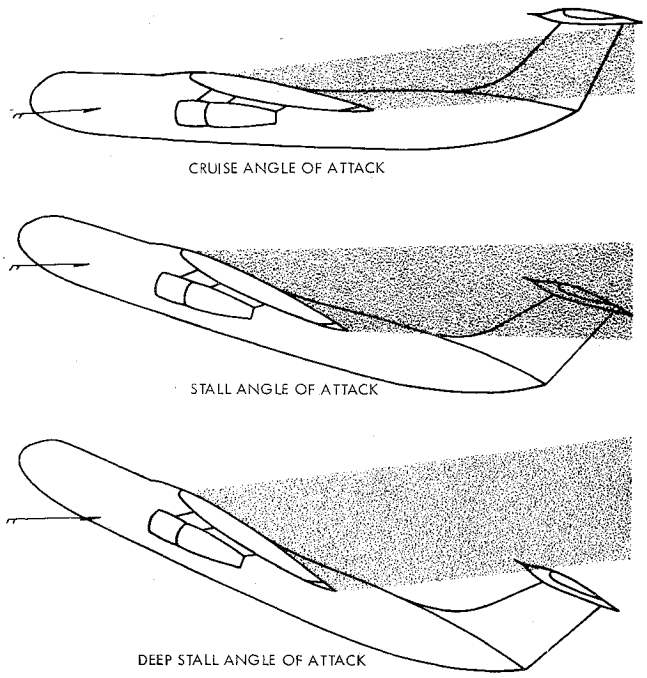

Fig. 7 Relationship of the horizontal tail to the turbulent wake of the wing.

The maximum vertical tail loads, and interface loads between the vertical and the horizontal tail, on the other hand, occurred when the flaps were down. This relationship is somewhat intuitive, since the horizontal tail (because of its location on top of the vertical fin) feeds in large bending and torsion moments when antisymmetric loadings are present.

Figure 8 shows a time history of a stall at a high angle of attack in the clean configuration, at an airspeed of approximately 160 knots and an altitude of 15,000 ft. The tip load factor and horizontal tail bending moment time histories are envelopes of the maximum measured values and make no attempt to show the actual load traces as a function of time due to the legibility problems that would be encountered. The peak angle of attack is 20.0°, and occurs at a point in time coincident with the peak load and load factor. The data shown in Figs. 6 and 8 represent the same stall, and indicate that the measured load levels between the 50% semi-span station and the tip exceed the design values by a significant margin.

Since the measured vertical tail load levels never exceeded the design limit strength of the structure, no time histories are shown. Also, comparative wind-tunnel data are available only in the clean configuration. For this reason, the discussions that follow are limited to the clean configuration, although there is no reason to believe that the results would be any different for other configurations.

Reproducing the Measured Loads

Various methods were tried in attempting to analytically reproduce the measured horizontal tail loads. One method consistently gave good results. This involved combining quasi-static airloads at the peak angle of attack with inertia loads resulting from application of the measured tip load factors to unit inertias derived from the 7.0-cps symmetrical bending mode shape of the horizontal tail. The quasi-static airloads are calculated by conventional means as indicated by Eqs. (5–9) and distributed uniformly without the application of arbitrary distribution factors:

$$C_{L_t} = (\alpha_{FRL} - \epsilon + i_t)C_{L\alpha_t} + \delta_e C_{L\delta_e} \tag{5}$$

$$(cc_l/c_{av})_\eta = (cc_{l_b}/c_{av})_\eta + C_{L_t}\,(cc_l/C_{L_t}\,c_{av})_\eta \tag{6}$$

$$S_{Z_\eta} = \frac{qS}{2}\int_1^0 \left(\frac{cc_l}{c_{av}}\right)_\eta d\eta \tag{7}$$

$$M_{X_\eta} = \frac{b}{2}\int_1^0 (S_Z)_\eta\, d\eta \tag{8}$$

$$M_{Y_\eta} = \frac{qS}{2}\int_1^0 \left(\frac{cc_l}{c_{av}}\right)_\eta \times \left(\frac{\Delta X}{\bar{C}}\right)_\eta d\eta \tag{9}$$

The unit inertias are obtained by applying the following equations where $(n_z)_\eta$ is obtained from Fig. 9:

$$\left(\frac{S_Z}{\Delta n_{z_{tip}}}\right)_\eta = \sum_1^0 (W)_\eta \times (n_z)_\eta \tag{10}$$

$$\left(\frac{M_X}{\Delta n_{z_{tip}}}\right)_\eta = \int_1^0 \left(\frac{S_Z}{\Delta n_{z_{tip}}}\right)_\eta d\eta \tag{11}$$

$$\left(\frac{M_Y}{\Delta n_{z_{tip}}}\right)_\eta = \sum_1^0 (W)_\eta \times (\Delta X)_\eta\,(n_z)_\eta \tag{12}$$

The net horizontal tail shear, bending, and torsion then become

$$S_{Z_{net_\eta}} = S_{Z_\eta} + \Delta n_{z_{tip}}(S_Z/\Delta n_{z_{tip}})_\eta \tag{13}$$

$$M_{X_{net_\eta}} = M_{X_\eta} + \Delta n_{z_{tip}}(M_X/\Delta n_{z_{tip}})_\eta \tag{14}$$

$$M_{Y_{net_\eta}} = M_{Y_\eta} + \Delta n_{z_{tip}}(M_Y/\Delta n_{z_{tip}})_\eta \tag{15}$$

Figure 10 shows a comparison of the flight-measured and derived bending moments for a typical stall at an airspeed of 160 KEAS, and an altitude of 15,000 ft. The shear and torsion comparisons are similar.

The statistical evidence compiled from a large number of comparisons similar to that shown in Fig. 10 strongly indicates that horizontal tail loads due to stall buffet can be satis-

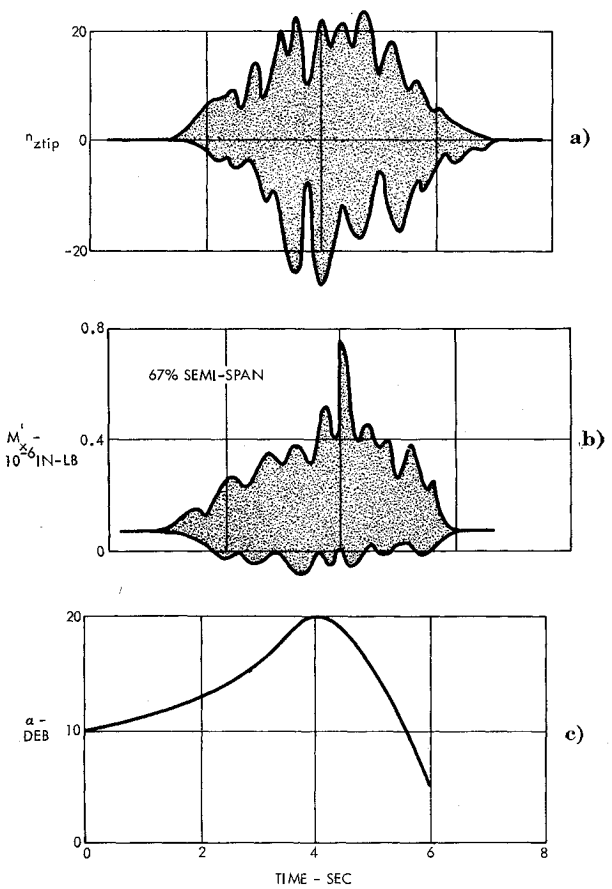

Fig. 8 Time history of a high-angle-of-attack stall in the clean configuration.

factorily characterized by a combination of quasi-static airload and incremental inertia loads. It remains then to establish a method of predicting horizontal tail tip load factors and peak airplane angles of attack before a rational method of loads computation can be derived.

Peak Angle-of-Attack Prediction

Many modern day aircraft are equipped with devices that either positively limit the airplane angle of attack, or warn the pilot of impending stall. The C-141, for instance, has both, a stick-shaker, which warns the pilot, and a stick-pusher, which pushes the airplane nosedown if the pilot ignores the warning. In the case of the C-141, mutual consent of Lockheed and the procuring agency established the angle of attack at which the stick-pusher actuation occurs as the peak angle of attack for consideration. Since this precedence has been established and thus far has proven satisfactory for the C-141, it would appear that the same reasoning could be applied to future airplanes.

Airplanes that are not equipped with such devices present somewhat of a problem. There are several bases that could be used in determining the peak angle of attack for consideration, but the choice of any one of them would be dependent upon the characteristics of the particular airplane being considered: 1) the angle of attack for maximum lift; 2) a rationally calculated angle of attack in excess of that for maximum lift; and 3) experience.

The use of basis 1 is probably the most logical for large transport airplanes, since the possibility of significantly exceeding the angle of attack for maximum lift is remote in the operations for which such an airplane is designed. Basis 2 is suggested as an alternate to 1. The peak angle of attack could be rationally calculated by a suitable dynamic analysis using predicted stability characteristics and assuming that the pilot begins his recovery at the angle of attack for maximum lift. Basis 3 implies the use of experience gained during flight tests of similar airplanes.

Actually, since the stall characteristics vary so significantly with the configuration of a given airplane, it may well be imprudent to even attempt to write an all-inclusive statement into the criteria regarding peak angle of attack. It is suggested therefore, that the choice of peak angle of attack be left open to joint agreement between the contractor and the procuring agency.

Rational Prediction of Empennage Buffet Loads

The method that was used to reproduce the flight test measured loads involved the superposition of quasi-static and analytically predicted airloads, and incremental inertia loads based on measured horizontal tail tip load factors. Prediction of the quasi-static airloads presents no problem once the peak angle of attack for consideration has been

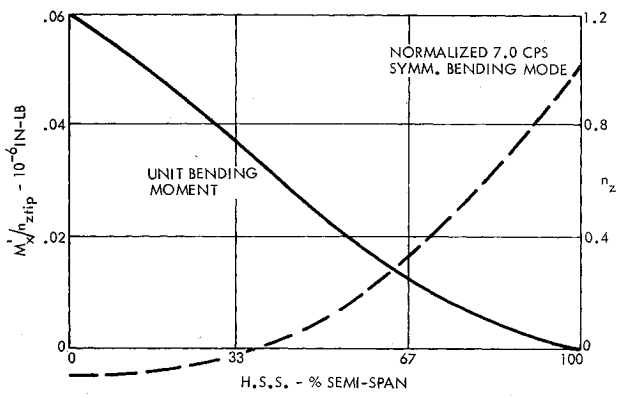

Fig. 9 Distribution of unit inertia bending moment and load factor.

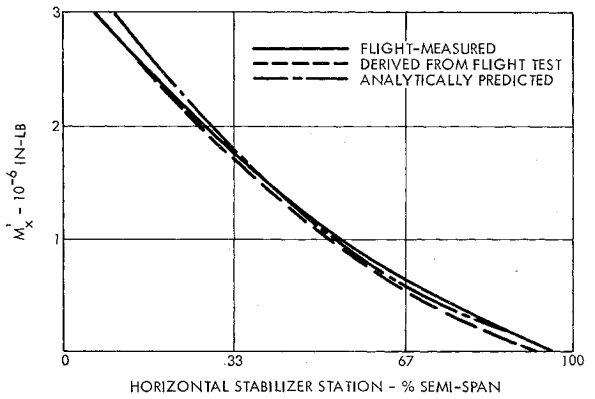

Fig. 10 Comparison of flight-measured and flight test derived horizontal tail bending moments.

established, since aerodynamic data are normally readily available for this purpose. Horizontal tail tip load factors and horizontal tail response modes resulting from stall buffet have not been available in the past, however, since a need for these was not recognized. For this reason, Lockheed initiated a wind-tunnel investigation of a $\frac{1}{24}$th scale flutter model of the C-141 in a low-speed tunnel in order to see whether such a model could be depended upon to predict these parameters. The results were very encouraging.

The model used was dynamically scaled to represent an altitude of 15,000 ft. The test procedure involved holding the wind-tunnel speed and model angle of attack constant for 20 sec while time histories of tip load factor were recorded on magnetic tape and direct writing records. The airplane angle of attack was varied from $-6°$ to $+20°$. Tests were conducted at scaled airplane speeds of 104, 155, and 207 KEAS.

Figure 11 shows the results of the wind tunnel tests in terms of tip load factor as a function of airplane angle of attack. Figures 12 and 13 show comparison of flight-measured and wind-tunnel predicted tip load factors at airspeeds of 133 and 170 KEAS, respectively. The wind-tunnel data indicate peak tip load factors which are three to four g's higher than the flight-measured values. The wind-tunnel data also indicate that the tip load factors begin to build up at a lower angle of attack than flight-measured data.

The discrepancies between the flight-measured and wind-tunnel tip load factors do not have an appreciable effect on

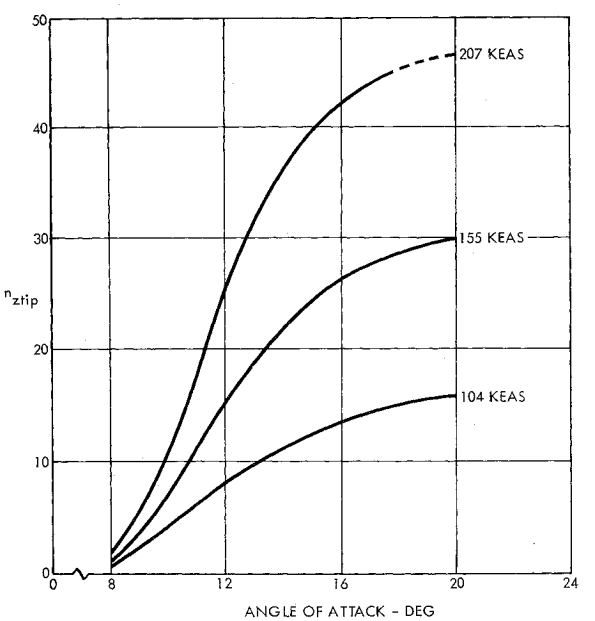

Fig. 11 Wind-tunnel predicted horizontal tail tip load factors.

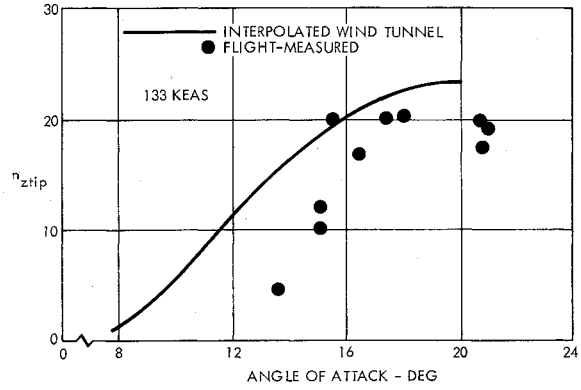

Fig. 12 Comparison of wind-tunnel predicted and flight-measured tip load factors.

the net horizontal tail load, as shown by Fig. 14. In fact, the wind-tunnel data coincidentally show a somewhat better over-all comparison with the flight-measured load.

Rationalization of Data Discrepancies

The discrepancies between the C-141 flight-measured and wind-tunnel predicted tip load factors cannot be conclusively explained; nevertheless, some rationalization is possible. The slightly higher peak load factors can probably be attributed to the necessity of clipping the model wing tips in order to fit the wind tunnel, or the method of conducting the tests. Clipping the wing tips may have increased the energy level in the wing wake at the empennage by moving the tip vortices inboard to a point where they impinged upon the horizontal stabilizer, thus causing greater excitation of the structure and higher load factors. The method of conducting the wind-tunnel tests, which involved a 20-sec stabilization at each angle of attack, may not have been a completely satisfactory representation of the airplane environment. The flight-measured data show some indication that the magnitude of the tip load factors is influenced by the length of time that the empennage is submersed in the turbulent wake of the wing. A better representation might be obtained by minimizing the time duration for each run or by actually cycling the model angle of attack in a manner similar to the actual maneuver.

The discrepancy in the angle of attack at which the load factor build-up begins can probably be attributed to the low Reynolds number of the wind-tunnel data. The model

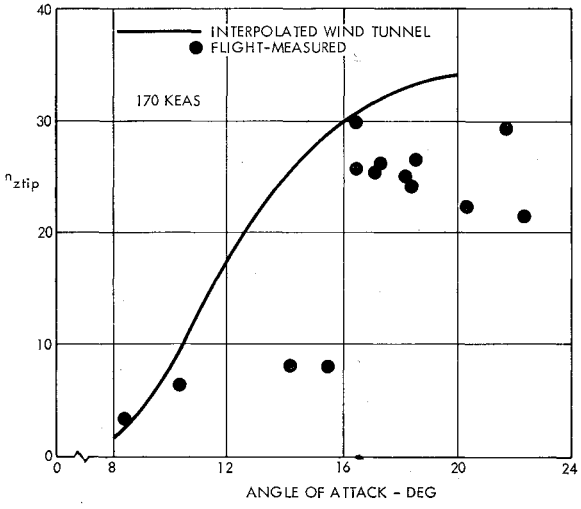

Fig. 13 Comparison of wind-tunnel predicted and flight-measured tip load factors.

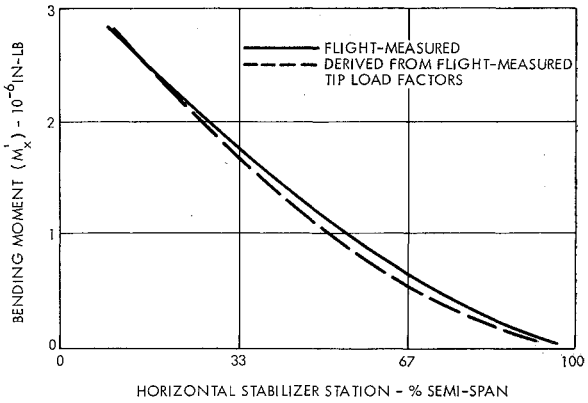

Fig. 14 Comparison of flight-measured, flight-derived, and analytically predicted horizontal tail bending moments.

Reynolds number was 300,000 compared to a full-scale Reynolds number of 30,000,000; this difference causes the model to stall at a lower angle of attack than the full-scale airplane.

Additional Research

The questions introduced by the apparent discrepancies between the flight-measured and wind-tunnel data point out a need for additional research. The absence of comparative wind-tunnel data in other configurations, such as flaps down, or spoilers deployed, also necessitates additional research.

Some evaluation of airplanes with different horizontal tail locations must also be made in order to insure that the method is universally acceptable. It is suggested that tests of models with horizontal tails mounted on the fuselage, and at the midspan of the vertical fin, in addition to the C-141 T-tail configuration, will satisfy this need. Comparative flight test data must also be obtained for airplanes other than the C-141.

Conclusions

Several conclusions can be drawn from the preceding discussions:

1) The military requirement for abrupt checked pitch maneuvers should be reworded in order to obtain compatibility between the design and flight test requirements. The requirement for coincidence of peak load factor and elevator return should be eliminated.

2) A re-evaluation, in the form of additional research, of arbitrary unsymmetrical horizontal tail load distribution factors is needed in order to obtain a better representation of the actual loads which occur in flight.

3) The requirement for an arbitrary center of gravity tolerance band should be replaced by a rational analysis.

4) The traditional method of establishing flight test zeros should be refined to utilize in-flight base points determined by experimental flight testing.

5) Wind-tunnel testing in a low Reynolds number range cannot be depended upon to produce realistic full-scale values of aerodynamic center and c_{mc} with contemporary methods of fixing transition. Additional research is needed to find better ways of fixing transition or obtaining a higher Reynolds number.

6) Prediction of empennage buffet loads by combining quasi-static, symmetricallly distributed airloads with incremental inertia loadings derived from wind-tunnel measured tip load factors offers a great deal of promise. Additional research is needed in order to demonstrate a universal application of the method.